ChemistrySelect

Research Article
doi.org/10.1002/slct.202400701

Chemistry Europe
European Chemical Societies Publishing

www.chemistryselect.org

In Silico and In Vitro Antifungal Investigations of Verbascoside Isolated From *Verbascum Ozturkii*

Samed Şimşek,[a] Hüseyin Akşit,[b] Yusuf Bayar,*[c] and Tuncay Karakurt[d]

This study investigates the antifungal properties of verbascoside isolated from *Verbascum ozturkii*. The primary objective is to evaluate its efficacy against two agriculturally significant plant pathogens, *Phytophthora infestans* and *Verticillium dahliae*. Verbascoside was isolated using preparative high-performance liquid chromatography (HPLC) and its structure was elucidated via nuclear magnetic resonance (NMR) spectroscopy. In vitro antifungal assays demonstrated moderate inhibitory effects with verbascoside (2 mg/mL) reducing mycelial growth by 23.49% for *P. infestans* and 19.42% for *V. dahliae*. To elucidate the antifungal mechanism, quantum chemical calculations and molecular docking studies were conducted. Analyses of frontier molecular orbitals (HOMO-LUMO) and molecular electrostatic potential (MEP) identified critical interaction sites. Molecular docking demonstrated that verbascoside binds favorably to the protein structures of *V. dahliae* (PDB: 5xmz) and *P. infestans* (PDB: 6jyg). Molecular dynamics simulations confirmed the stability of these interactions with molecular mechanics Poisson-Boltzmann surface area (MM/PBSA) calculations indicating more favorable binding free energy for the verbascoside-6jyg complex. This research underscores the potential of verbascoside as a natural antifungal agent highlighting the significance of protein-specific interactions. The findings contribute to the development of alternative antifungal strategies and emphasize the novelty of verbascoside activity against these plant pathogens.

1. Introduction

The Verbascum genus commonly referred to as "sığırkuyruğu" in Türkiye is a member of the Scrophulariaceae family representing 360 species worldwide. Notably, 245 of these species are endemic to Türkiye demonstrating a high endemism rate by 80%.[1] Verbascum species hold significant value in traditional medicine and aromatherapy primarily used as expectorants, mucolytics, and sedatives for the treatment of respiratory disorders such as bronchitis, tuberculosis-related dry cough, and asthma.[2,3] Furthermore, these species exhibit diuretic, sedative, anti-inflammatory, and relaxing properties on the urinary tract and are traditionally used in the treatment of hemorrhoids, rheumatic pain, superficial fungal infections, wounds, and diarrhea.[1] Verbascum species contain a variety of biologically active secondary metabolites, saponins,[4] flavonoids,[5] iridoids,[6] and phenylethanoids,[7] which exhibit diverse biological activities. Phenylethanoid glycosides, a key group of natural products in Verbascum, have garnered increasing interest due to their significant role in the prevention and treatment of various human diseases.[8–10]

V. ozturkii Karavel., Uzunh & S.Celik sp. nov. (Sect. Bothrosperma Murb.) is a biennial endemic herb from Türkiye primarily grown in Erzincan. This species, known as "öztürk sığırkuyruğu", grows to a height of 30–60 cm and is characterized by dense stellate and sparsely stalked glandular features.[11] To the best of our knowledge, no studies in the literature have investigated the chemical composition and biological activity of *V. ozturkii*. In this study, we developed selective extraction and reproducible isolation methods using preparative HPLC to purify verbascoside, which is reported here for the first time.

Verbascoside, the most common phenylethanoid in the genus Verbascum exhibits a range of biological activities including antioxidant, anti-inflammatory, cholinesterase inhibitory, and cytotoxic effects.[12–16] Additionally, in traditional medicine plants containing verbascoside have been used to treat inflammation and microbial infections.[17] Several studies have reported its antifungal activity against pathogens such as *Cryptococcus neoformans*, *Fusarium culmorum*, *Bipolaris sorokiniana*, *Penicillium digitatum*, and *Candida species*.[18–21] However, its antifungal activity against *P. infestans* and *V. dahliae* remains underexplored. Both pathogens cause significant crop losses especially in potato and tomato fields where commonly used chemical control methods include fungicides like azoxystrobin, mefenoxam, and fludioxonil. Nevertheless, the detrimental impacts of these chemicals on human health and the environment have driven researchers to explore alternative strategies. Exploring plant-derived bioactive compounds holds promise for the discovery

[a] S. Şimşek
Medical Services and Techniques Dept. Çayırlı Vocational School, Erzincan Binali Yıldırım University, Erzincan 24500, Türkiye

[b] H. Akşit
Faculty of Pharmacy, Analytical Chemistry Dept., Erzincan Binali Yıldırım University, Erzincan 24100, Türkiye

[c] Y. Bayar
Faculty of Agriculture, Plant Protection Dept., Kırşehir Ahi Evran University, Kırşehir 40100, Türkiye
E-mail: yusuf.bayar@ahievran.edu.tr

[d] T. Karakurt
Faculty of Engineering-Architecture, Chemical Engineering Dept., Kırşehir Ahi Evran University, Kırşehir 40100, Türkiye

Supporting information for this article is available on the WWW under https://doi.org/10.1002/slct.202400701

of novel natural antifungal agents to manage pathogenic fungi more eco-friendly.[9]

This research is the first to examine the antifungal effect against *V. dahliae* and *P. infestans* properties of verbascoside. The computational modeling of ligand-protein interactions within the complex structure formed between verbascoside and the receptor was conducted using Molecular Docking. This approach allowed the identification of the binding poses and the interaction profiles of verbascoside with the active sites of the selected receptors. Additionally, molecular dynamics (MD) simulations were performed to thoroughly analyze the molecular interactions, binding mechanisms, stability, energy profile of the complex structure, and structural changes occurring between the ligand and protein over time. Experimentally, the ligand verbascoside was tested in vitro for its effects on *P. infestans and V. dahliae*, two pathogenic fungi responsible for significant agricultural losses. Based on these experimental results, the receptor structures associated with these fungi, 5xmz and 6jyg were selected for computational studies. These receptors, which include co-ligands bound to their active sites represent biologically relevant conformations. Verbascoside was docked into the active binding regions of these receptors preserving their co-ligand interactions to ensure realistic binding scenarios. Subsequently, molecular dynamics simulations were employed to provide deeper insights into the ligand's binding stability and its potential effects on the structural dynamics of the receptors. These simulations revealed critical details regarding the adaptability of verbascoside within the active binding regions and its energetic compatibility with the receptor-ligand complex. This integrated approach combining docking and MD simulations highlights the binding efficiency of verbascoside and its potential role as an inhibitor for fungal pathogens.

Therefore, the objective of the current study is to evaluate the antifungal potential of verbascoside against *V. dahliae* and *P. infestans* for the first time as well as to explore the molecular interactions, binding mechanism, and stability of the ligand-protein interactions using computational modeling, molecular docking, and molecular dynamics simulations.

2. Experimental Section

2.1. Plant Material

The aerial parts of *V. ozturkii* were collected from the Bağıştaş Village in İliç, Erzincan, Türkiye in June 2020. The authentication of the plant sample was carried out by Prof. Dr. Ali Kandemir from the Department of Biology, Faculty of Art and Science, University of Erzincan Binali Yıldırım. A voucher specimen with the identification number KANDEMIR-10574 was deposited in the EBYU Herbarium for future reference and verification.

2.2. Preparative HPLC Conditions

The purification of verbascoside was achieved using a Shimadzu Prominence semipreparative HPLC equipped with an LC20AR pump, SPD-20A UV detector, FRC-10A fraction collector, and EMR Chrometsil C18 (250 × 20 mm, 10 µm) column. Deionized water (A) and acetonitrile (B) were used as the mobile phase with an 8 mL/min flow rate. Gradient elution starting from 90:10 (A: B) to 50:50 (A: B) for 30 min was applied to the separation of a target molecule. UV detection was performed at 235 and 280 nm.[1,22]

2.3. Extraction Procedure

The plant material (100 g) was thoroughly dried and finely ground. The ground material was then subjected to maceration with 500 mL of methanol for 3 h using an ultrasonic bath. This maceration process was repeated three times under identical conditions. The resulting mixture was filtered and the solvents were evaporated yielding a dark green semisolid crude extract (12 g). The extract was stored at 4 °C until used.

2.4. In Vitro Antifungal Activity

The antifungal activity of verbascoside was tested using the agar plate method.[23] Verbascoside was dissolved in DMSO and added to 60 mL of Potato Dextrose Agar (PDA) cooled to 40 °C resulting in a final concentration of 2 mg/mL. The PDA mixture was poured into 60 mm diameter petri plates at approximately 10 mL per plate. Fungus cultures including *P. infestans* and *V. dahliae* were obtained from the stock culture collection of Kırşehir Ahi Evran University, Faculty of Agriculture, Phytopathology Laboratories. The plant pathogens were grown on a PDA medium and incubated at 22 ± 2 °C for 7 days to prepare the fungal cultures for activity assays. Agar discs (5 mm) containing these fungal mycelia were transferred to the petri plates for testing. The fungal cultures were further incubated at 22 ± 2 °C for 14 days and the mycelial growth was recorded daily during this period. Control groups included the commercial fungicide Thiram (80% w/v) as a positive control and 1% (v/v) DMSO as a negative control. The experiment was conducted in triplicate for each condition and repeated twice to ensure reliability. The percentage of mycelial growth inhibition (MGI) was calculated according to the formula:[24]

$$MGI\% = 100 \times (dc - dt)/dc$$

where dc: the mycelial growth in the control group, dt: the mycelial growth in the treatment group

2.5. Molecular Docking

The optimization of the isolated verbascoside molecule and the calculation of some of its parameters were obtained using the B3LYP[25,26]method and the 6–31g(d)[27] basis set with the Gaussian 09[28]program (Figure 1). The obtained results were visualized with the help of GaussView 5[29] software. Docking simulations of the verbascoside ligand and protein structures were performed using Chimera[30] and Autodockvina[31] software.

2.6. Molecular Dynamics Simulation

Molecular dynamics simulations of the verbascoside compound with the data obtained as a result of the docking simulation were performed with the GROMACS[32] program. This program is used to understand and analyze the behavior of biomolecules such as proteins, nucleic acids, and lipids. GROMACS is open-source software that can run on high-performance computing (HPC) systems and can be used on many different platforms. Furthermore, GROMACS is

Research Article
doi.org/10.1002/slct.202400701

Chemistry Europe
European Chemical Societies Publishing

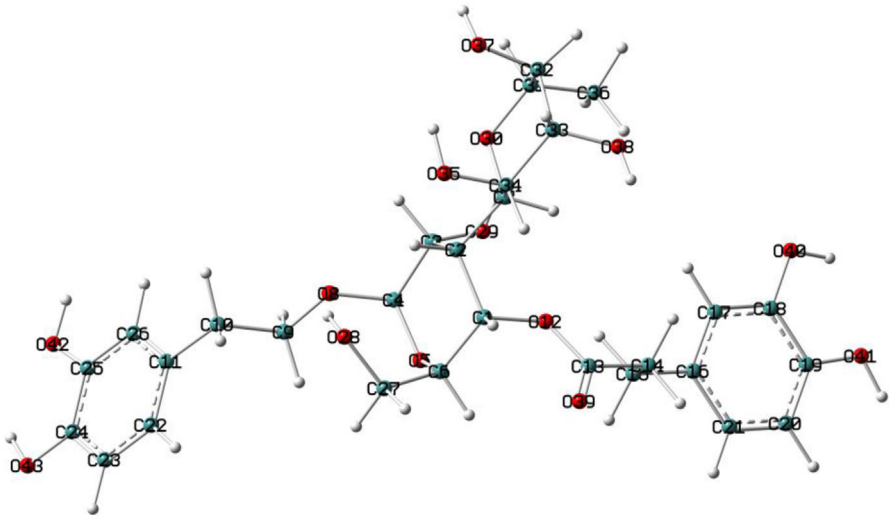

Figure 1. Optimized structure of verbascoside molecule.

a popular choice because it has a user-friendly interface and offers many different analysis tools. MD simulations were performed with the help of "GROMACS" software. With the "g_mmpbsa" module,[33] the binding energies in complex structures were calculated and the contribution of amino acids in the binding site to the binding on the ligand was analyzed.

3. Results and Discussion

3.1. Isolation of Verbascoside

The crude extract was dissolved in hot water and then cooled to room temperature. The nonsoluble components were removed by filtration to give the water-soluble fraction. The filtrate was subjected to lyophilization overnight to give a pale-yellow solid (6.4 g). A portion of the extract (2 g) was dissolved in 20 mL of deionized water and repeatedly injected into a preparative HPLC system over a 2 mL sample loop. Subsequently, fraction 3 (Figure S1) containing the target compound was subjected to further purification using a recycling mode with isocratic elution using a mixture of 60:40 (water: ACN). The recycling process was repeated until a distinct separation was achieved (Figure S2). After the sixth cycle the desired peak corresponding to the verbascoside was collected, yielding a quantity of 280 mg.

Verbascoside: ^{1}H NMR (400 MHz, MeOD) δ_H 7.62 (d, J = 15.8, 1H, Hβ''), 7.08 (d, J = 2.1, 1H, H2″), 6.98 (dd, J = 8.2, 2.1, 1H, H6″), 6.80 (d, J = 8.0, 1H, H5″), 6.72 (d, J = 2.1, 1H, H2), 6.70 (d, J = 7.9, 1H, H5), 6.59 (dd, J = 8.0, 2.1, 1H, H6), 6.30 (d, J = 15.9, 1H, Hα''), 5.21 (d, J = 1.8, 1H, H1‴″), 4.94 (m, 1H, H4‴′), 4.40 (d, J = 7.9, 1H, H1‴′), 4.07 (dt, J = 9.7, 7.3, 1H, Hαa), 3.94 (m, 1H, H2‴″), 3.84 (t, J = 9.2, 1H, H3‴′), 3.72–3.76 (m, 1H, Hαb), 3.65 (m, 1H, H6‴′a), 3.61 (m, 1H, H3‴″), 3.58 (m, 1H, H5‴″), 3.56 (m, 1H, H5‴′), 3.54 (m, 1H, H6‴′b), 3.41 (t, J = 8.5, 1H, H2‴′), 3.28–3.34 (m, 1H, H4‴″), 2.81 (dt, J = 7.4, 2.5, 2H, Hβ), 1.11 (d, J = 6.2, 3H, H6‴′′) (Figure S3). ^{13}C NMR (100 MHz, MeOD) δ_C 166.9 (C=O), 148.4 (C4″), 146.6 (Cβ''), 145.4 (C3″), 144.7 (C3), 143.3 (C4), 130.2 (C1), 126.3 (C1″), 121.8 (C6″), 119.9 (C6), 115.8 (C2), 115.2 (C5″), 114.9 (C5), 113.9 (C2″), 113.4 (Cα''), 102.8 (C1‴′), 101.6 (C1‴″), 80.3 (C3‴′), 74.8 (C2‴′), 74.6 (C5‴′), 72.4 (C4‴″), 71.0 (C2‴″), 70.9 (Cα), 70.7 (C3‴″), 69.3 (C4‴′), 69.0 (C5‴″), 61.0 (C6‴′), 35.2(Cβ), 17.1 (C6‴″) (Figure S4). The NMR assignments were fully in agreement with the literature.[1,22,34] Verbascoside, a common phenylethanoid found in various Verbascum species has previously been isolated from *V. speciosum*,[35] *V. undulatum*,[36] and *V. mucronatum*.[37] However, this study marks the first report on the isolation of verbascoside from *V. ozturkii* which is an endemic species found in Türkiye.

Table 1. Percent mycelium inhibition of verbascoside against test fungi in vitro conditions (%).

Test Fungi	Concentration (mg/mL)	% Mycelial Growth Inhibition
V. dahliae	C-	–
	2	19.42
	C+	100
P. infestans	C-	–
	2	23.49
	C+	100

(-) no activity

3.2. In Vitro Antifungal Activity

It has been reported that verbascoside has many biological and antimicrobial activities. The antifungal effects of verbascoside at 2 mg/mL concentrations are shown in Table 1. Verbascoside treatments significantly reduced the growth of *P. infestans* and *V. dahliae* compared to negative control. Although the application of verbascoside varies according to the test fungi, there is a noticeable antifungal activity at the applied concentrations. It was determined that the application dose inhibited the mycelial growth of *V. dahliae* and *P. infestans* by 19.42%

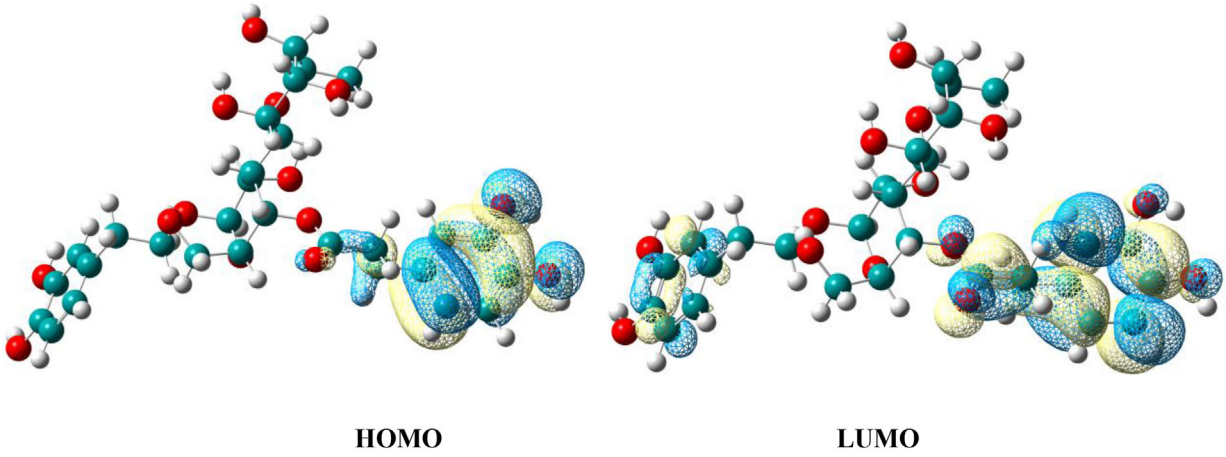

Figure 2. HOMO-LUMO orbitals of verbascoside molecule.

and 23.49%, respectively. In both pathogens 100% inhibition of mycelial growth was observed in the positive control.

In a study, it was reported that *Lippia javanica* and *Lantana camara* leaf extract containing 2.0 g/L verbascoside provided 90% and 100% protection, respectively when applied to *Penicillium digitatum* infected fruits.[38] In a similar study, the in vitro antifungal properties of verbascoside and verbascoside-rich extracts containing 0.6 g of verbascoside per 1 liter of solution were reported.[39]

3.3. Quantum Chemicals Activate Indicatives and Molecular Docking

Frontier orbits (HOMO-LUMO) and Molecular electrostatic potential (MEP) surface were calculated on the optimized verbascoside structure (Figure 1) to identify nucleophilic and electrophilic sites that will shed light on molecular docking studies. The HOMO (Highest Occupied Molecular Orbital) and LUMO (Lowest Unoccupied Molecular Orbital) orbitals are used to determine the chemical properties of a molecule. HOMO is the highest energy occupied molecular orbital in a molecule. This orbital is the highest energy level of electrons in a molecule and is the source of electrons in chemical reactions. The LUMO is the lowest energy empty molecular orbital in a molecule. The HOMO and LUMO orbitals are important factors that determine the reactivity of a molecule and play an important role in many different chemical reactions.[40] These orbitals are also used to determine the optical properties of a molecule. The surface of the FMOs can be used to interpret the binding framework of the calculated compound. As shown in Figure 2, the HOMO orbitals are localized around the O40, O41 atoms, and the benzene ring, while the LUMO orbitals are localized on the O40, O41, C14, C16, O12, O39 atoms and the benzene ring. These results suggest that O40, O41, C14, C16, O12, O39 atoms and benzene ring fragments may play important roles in antifungal activity.

Another method used to determine the active sites of the molecule is the Molecular electrostatic potential (MEP) surface map. This map can provide important information about the ligand molecule to be used in drug design.[41] Looking at the MEP map of the verbascoside molecule (Figure 3), the red color represents regions that are partially negative charge or electron-rich and the blue color represents regions that are partially positive charge or electron-deficient. Figure 3 shows that the negative regions are mostly located on O atoms and the positive regions are located on H atoms on O-H groups. This indicates that these atoms provide the primary interactions for strong hydrogen bonding through their electron-donating and electron-withdrawing properties.

In this study, the visualization of the ligand and the complex structure formed as a result of molecular docking was performed with BIOVA Discovery Studio Visualizer, 2019.

The 5xmz and 6jyg proteins were selected as targets in this study due to their biological significance and structural characteristics. This 5xmz plays a crucial role in [a specific biological pathway, such as signal transduction or metabolism] and its structure has been resolved at high resolution via crystallography. This ensures the reliability of the protein structure and provides a robust foundation for molecular modeling studies. Additionally, the well-defined active site makes it suitable for ligand binding analysis. In comparison to 5xmz, this 6jyg exhibits greater structural flexibility which allows for a broader investigation of ligand-binding conformations. Furthermore, 6jyg is associated with [a specific disease or biological pathway] making it a potential therapeutic target. Its structural features including accessible binding pockets make it advantageous for molecular dynamics simulations.

The ligand (verbascoside) used in this study has been experimentally tested in vitro for its effects on *P. infestans* and *V. dahliae*, two fungal pathogens responsible for significant agricultural losses. These findings formed the basis for selecting 5xmz and 6jyg receptors, as they are associated with the structures of *P. infestans* and *V. dahliae* providing a direct experimental justification for their use. In conclusion, the selection of these two proteins is scientifically justified based on their biological importance and the experimental validation provided.

The validation of the selected protein structures was performed using structural quality assessment tools including the

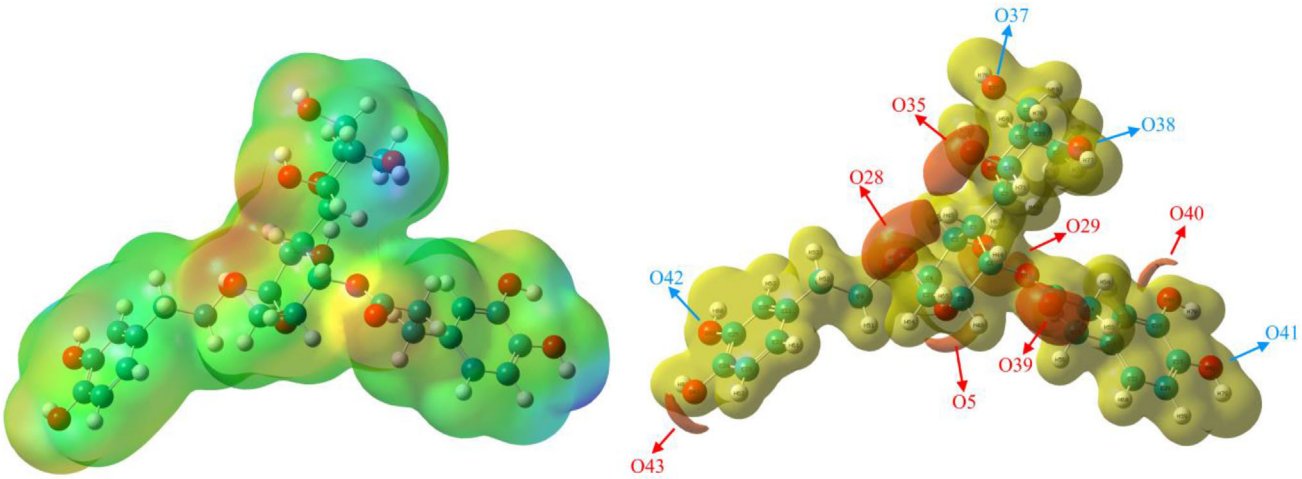

Figure 3. MEP Maps of verbascoside molecule.

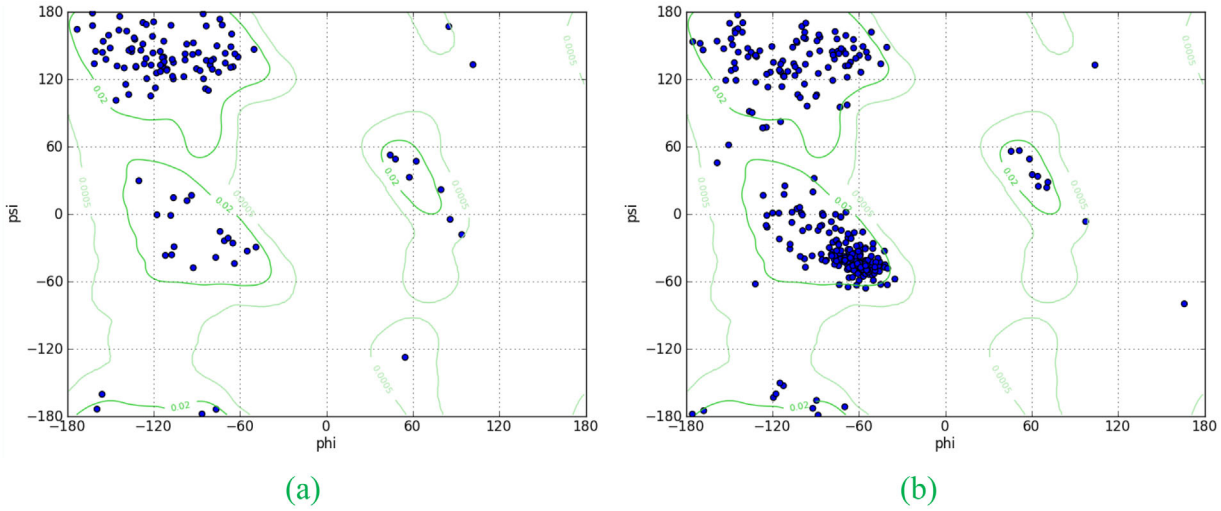

Figure 4. Ramachandran plots (a) **5xmz** (b) **6jyg** protein structures.

generation and analysis of Ramachandran plots (Figures 4a and 4b). These plots evaluate the backbone dihedral angles (φ and ψ) of the amino acid residues ensuring that the majority of residues fall within the allowed or favorable regions indicative of a high-quality protein structure.

For 5xmz, the Ramachandran plot shows:

Majority of residues (above 90%) are located in the most favorable regions, particularly in α-helix and β-sheet conformations, confirming its structural stability.

For 6jyg, the Ramachandran plot indicates:

A slightly higher level of flexibility with the majority of residues in the favorable regions and a small proportion in the allowed regions which aligns with the structural features required for conformational adaptability.

Protein crystal structures of *V. dahliae* (PDB:5xmz) and *P. infestans* (PDB:6jyg) were downloaded from the Protein Data Bank (PDB; www.rcsb.org). Preparation of the ligand and proteins for docking was performed using the Chimera program and protein docking was performed using the Autodockvina module The verbascoside molecule was successfully docked into the active site of both proteins (Figure 5a and 6a).

The nucleotides in the binding site of the 5xmy protein are LYS58, ASP120, ARG60, TYR86, TYR86, and PRO119, while those of the 6jyg protein are GLY10, THR9, GLN11, VAL47, ASP46, SER70, ILE12, ILE34, LEU72, ALA69 and VAL86. LYS58, ASP120, and ARG60 nucleotides of 5xmy protein formed three hydrogen bonds with O4, O11, and H38 atoms of the ligand, while TYR86 and PRO119 nucleotides formed hydrophobic interactions (Table 2). The π—π stacking interaction between TYR86 nucleotide and ligand is formed in a T-shaped form (Figure 4b).

The nucleotides in the binding site of 6jyg protein are GLY10, GLN11, VAL47, ASP46, SER70, ILE12, ILE34, LEU72, ALA69, VAL47, VAL8 (Table 3). Five hydrogen bonds were formed between the nucleotides GLY10, GLN11, VAL47, ASP46, and SER70 of the protein and O2, O12, and O13 atoms of the ligand. Six π-alkyl interactions occurred between the nucleotides ILE12, ILE34, LEU72, ALA69, VAL47, and VAL86 and the ligand (Figure 5b). The 2D interactions of both complex structures are also shown in Figure 4c and 5c.

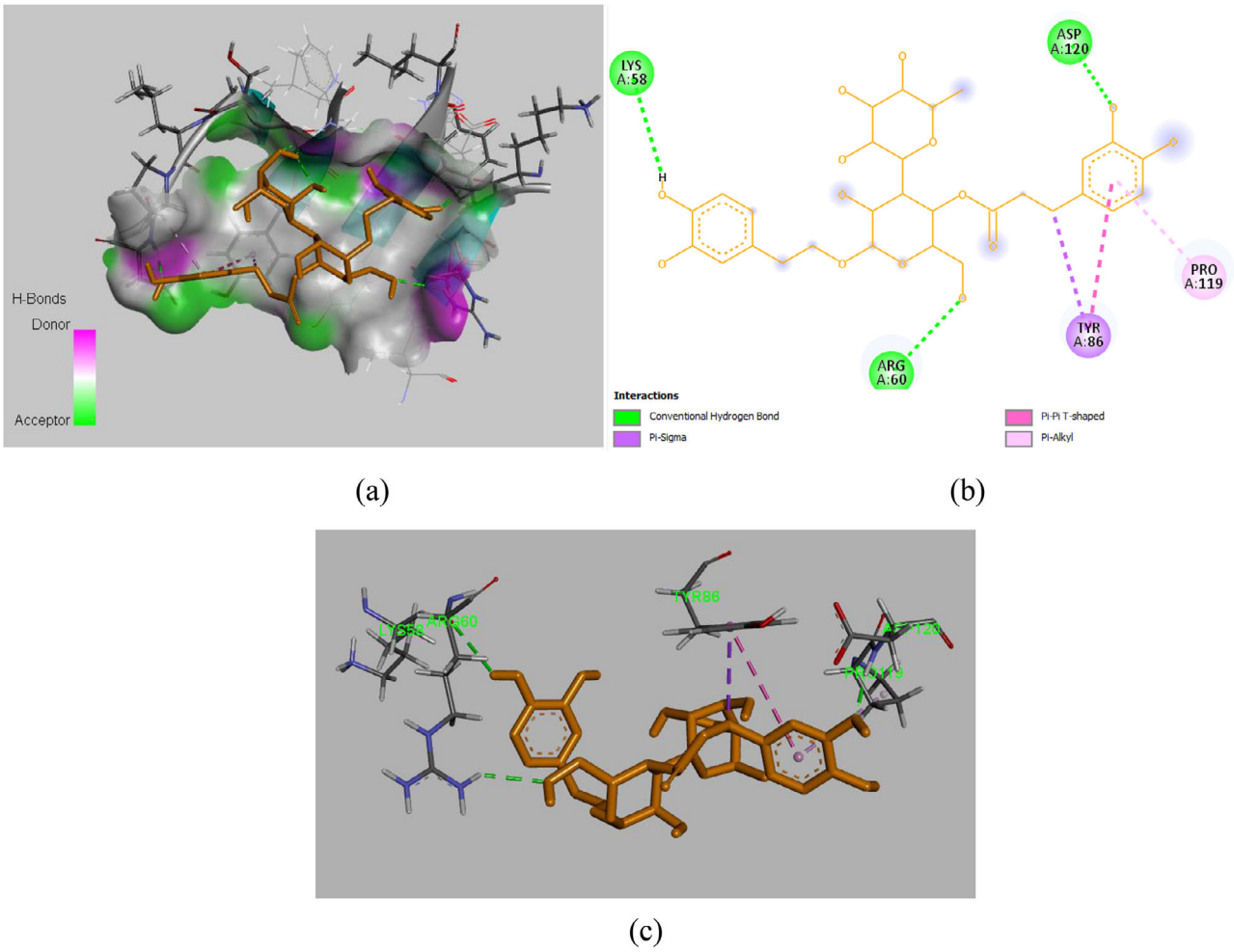

Figure 5. (a) The position of the verbascoside ligand located in the active site of the 5xmz protein in the complex structure mapped with the electrostatic potential and (b) 2D ligand-receptor interaction diagram (c) Binding interaction of ligands with amino acid residues of the target.

3.4. Molecular Dynamics

First the verbascoside molecule bound to the receptor as a result of molecular docking was converted into a "mol" format by making charge distributions in Chimera software. The creation of the topology file and the preparation of the parameters for molecular dynamics simulation were done with the Amber18[42] software. Using the Antechamber program, a module of the Amber18, the parameters of the molecule that determine the properties of the molecule such as atom type, charge, bond lengths, and angles were calculated. This information includes the properties of the molecule, the solvent environment, and other parameters. After determining the parameters, a topology file for the molecule was created using the "parmchk2" command. This file contains the force field parameters of the molecule. After creating the topology file, the "tleap" command was used to create the force field (amber99 sb) parameters of the molecule and other files needed to run a simulation. Molecular dynamics simulations were performed with the GROMACS program. The system defined as a cubic box contains the complex formed with dimensions $x = 12$ nm, $y = 12$ nm, and $z = 12$ nm. The TIP3P water model was chosen for the solution of the box under periodic boundary conditions. The systems were also brought to equilibrium by neutralizing with 9 (verbascoside-5xmz) and 11 Na^+ (verbascoside-6jyg) ions (Figure 7).

The energy minimization of the systems was performed using the steepest-descent algorithm in 764 steps for the 5xmz-verbascoside complex and 456 steps for the 6jyg-verbascoside complex. The potential energy changes of the systems are presented in Figure 8. It is seen that the potential energies fluctuate between −100000 kJ/mol and −450000 kJ/mol and between −100000 kJ/mol and −700000 kJ/mol for the 5xmz-verbascoside and 6jyg-verbascoside complexes, respectively and the systems reach stable values around −450000 kJ/mol and 650000 kJ/mol.

Using the NPT (Number-Pressure-Temperature) condition set, the simulation was performed where the pressure and temperature were kept constant after energy minimization of both systems. The system temperatures are maintained at 300 K on average with a 0.1 ps time constant v-rescale thermostat, while the system pressure is kept constant at 1 bar with a Berendsen barostat. Simulations were performed using periodic boundary conditions and the time step was taken as 10000 ps. Based on the four parameters, the stability of the complexes was ana-

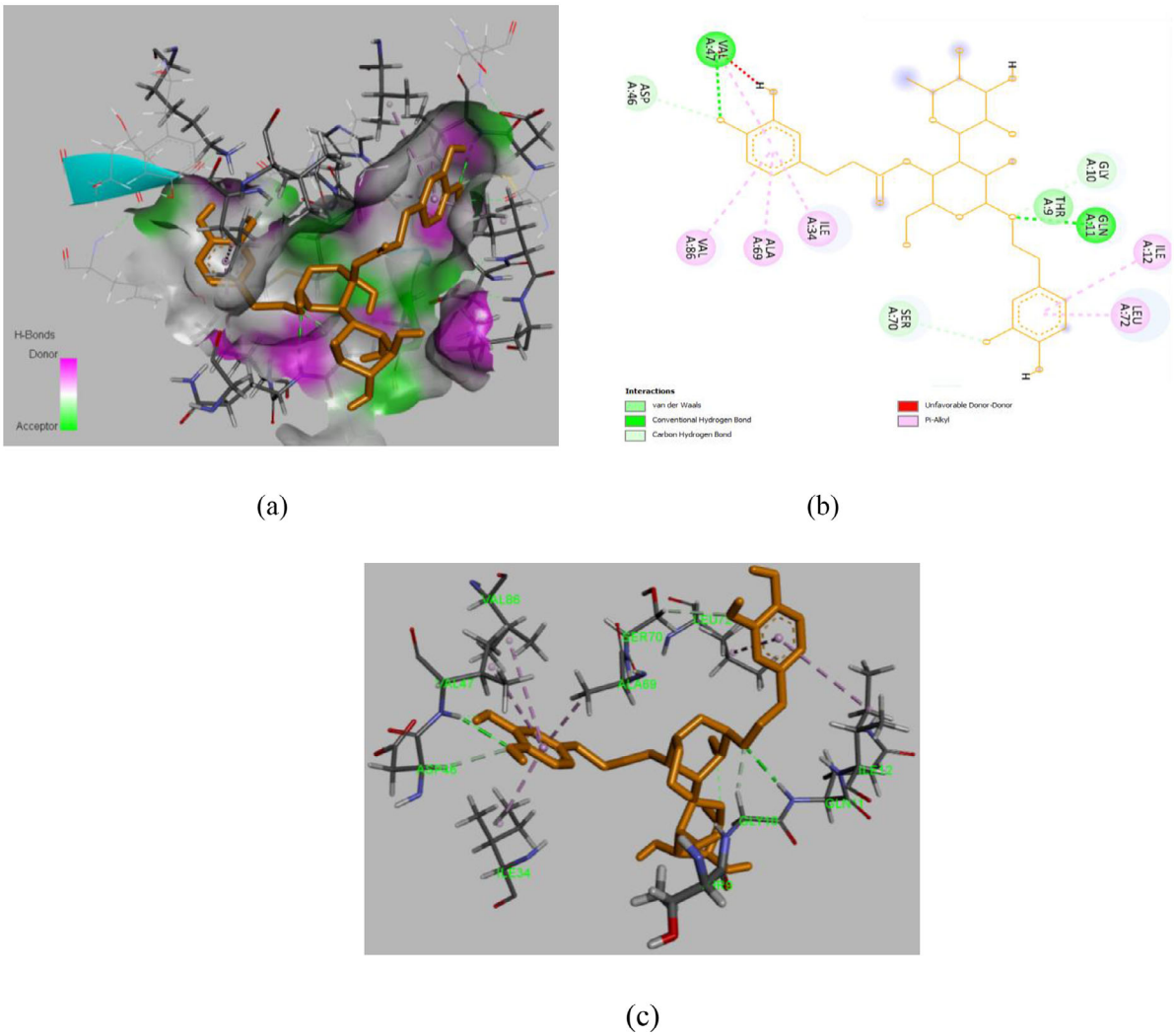

Figure 6. (a) The position of the verbascoside ligand located in the active site of the 6jyg protein in the complex structure mapped with the electrostatic potential and (b) 2D ligand-receptor interaction diagram (c) Binding interaction of ligands with amino acid residues of the target.

Table 2. Interactions between verbascoside and 5xmz receptor.

Donor group	Interaction Distance (Å)	Interaction Category	Interaction Types	Donor Group	Acceptor Group Types	Acceptor Group	Acceptor Group Types	Donor-H Acceptor Angle (°)
A:ARG60:HH12 – A:UNK1:O4	2.62	Hydrogen Bond	Conventional Hydrogen Bond	A: ARG60:HH12	H-Donor	A: UNK1:O4	H-Acceptor	130.164
A:ASP120:HN – A:UNK1:O11	1.96	Hydrogen Bond	Conventional Hydrogen Bond	A: ASP120:HN	H-Donor	A: UNK1:O11	H-Acceptor	165.4
A:UNK1:H38 – A:LYS58:O	3.01	Hydrogen Bond	Conventional Hydrogen Bond	A: UNK1:H38	H-Donor	A: LYS58:O	H-Acceptor	132.805
A:UNK1:C12 – A:TYR86	3.71	Hydrophobic	Pi-Sigma	A: UNK1:C12	C-H	A: TYR86	Pi-Orbitals	
A:TYR86 – A:UNK1	5.48	Hydrophobic	Pi-Pi T-shaped	A: TYR86	Pi-Orbitals	A: UNK1	Pi-Orbitals	
A:UNK1 – A:PRO119	5.40	Hydrophobic	Pi-Alkyl	A: UNK1	Pi-Orbitals	A: PRO119	Alkyl	

lyzed by Root-mean-square deviation (RMSD), Radius of gyration (R_G), Root-mean-square fluctuation (RMSF), and Solvent accessible surface area (SASA) through molecular dynamics simulation. RMSD is a method used to measure the structural similarity between two molecules. RMSD docking is often used to find stable conformations of protein-protein, protein-ligand, and other biological complexes. It is a method frequently used in molecular modeling and drug design studies. This method is a powerful tool for assessing the quality of protein-ligand interactions and is widely used in areas such as drug discovery and the study

Table 3. Interactions between verbascoside and *6jyg* receptor.

Donor Group	Interaction Distance (Å)	Interaction Category	Interaction Types	Donor Group	Acceptor group Types	Acceptor Group	Acceptor Group Types	Donor-H Acceptor Angle (°)
A:GLN11:HN –:UNK1:O2	2.26	Hydrogen Bond	Conventional Hydrogen Bond	A: GLN11:HN	H-Donor	: UNK1:O2	H-Acceptor	138.678
A:VAL47:HN –:UNK1:O12	2.41	Hydrogen Bond	Conventional Hydrogen Bond	A: VAL47:HN	H-Donor	: UNK1:O12	H-Acceptor	132.622
A:GLY10:HA2 –:UNK1:O2	2.30	Hydrogen Bond	Carbon Hydrogen Bond	A: GLY10:HA2	H-Donor	: UNK1:O2	H-Acceptor	138.548
A:ASP46:HA –:UNK1:O12	2.74	Hydrogen Bond	Carbon Hydrogen Bond	A: ASP46:HA	H-Donor	: UNK1:O12	H-Acceptor	135.169
A:SER70:HB1 –:UNK1:O13	2.92	Hydrogen Bond	Carbon Hydrogen Bond	A: SER70:HB1	H-Donor	: UNK1:O13	H-Acceptor	125.022
:UNK1 – A:ILE34	3.88	Hydrophobic	Pi-Alkyl	: UNK1	Pi-Orbitals	A: ILE34	Alkyl	
:UNK1 – A:VAL47	5.34	Hydrophobic	Pi-Alkyl	: UNK1	Pi-Orbitals	A: VAL47	Alkyl	
:UNK1 – A:ALA69	3.96	Hydrophobic	Pi-Alkyl	: UNK1	Pi-Orbitals	A: ALA69	Alkyl	
:UNK1 – A:VAL86	5.44	Hydrophobic	Pi-Alkyl	: UNK1	Pi-Orbitals	A: VAL86	Alkyl	
:UNK1 – A:ILE12	5.32	Hydrophobic	Pi-Alkyl	: UNK1	Pi-Orbitals	A: ILE12	Alkyl	
:UNK1 – A:LEU72	4.52	Hydrophobic	Pi-Alkyl	: UNK1	Pi-Orbitals	A: LEU72	Alkyl	

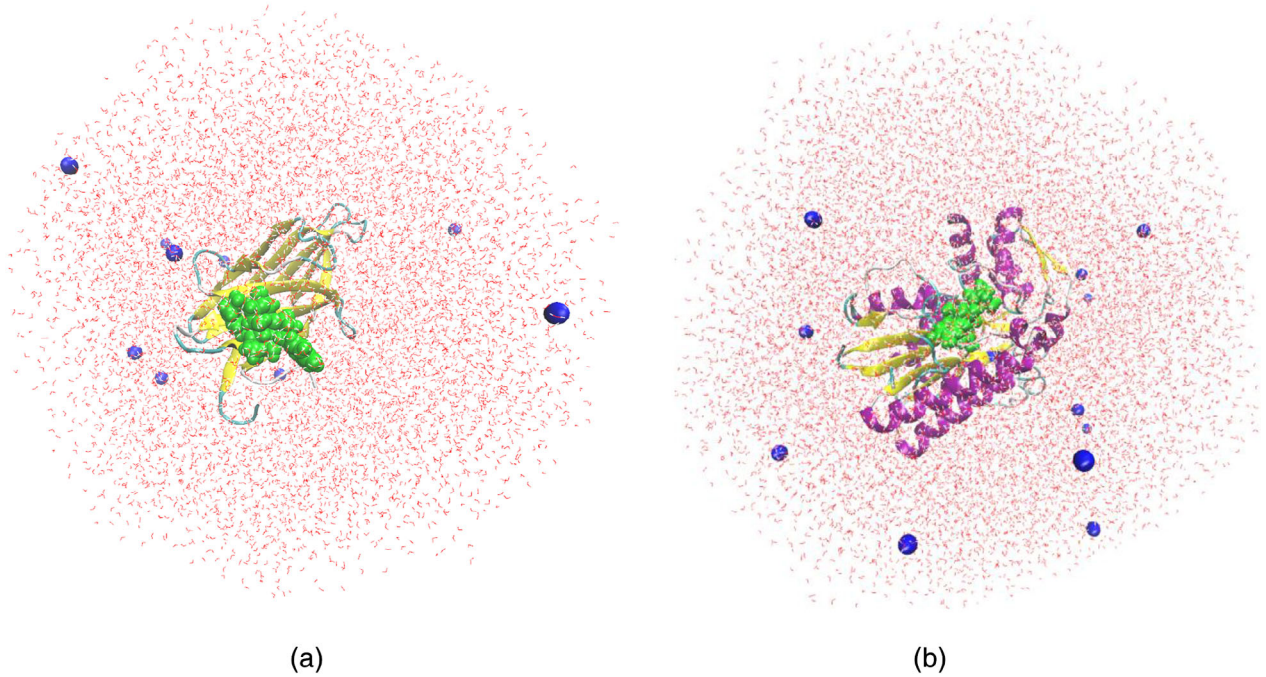

Figure 7. The systems (a) verbascoside-5xmz (b) verbascoside-6jyg filled with water, neutralized with Na^+(blue) ions and ligand (green).

of protein-ligand interactions. In the simulation results, it was observed that the ligand in the 5xmz-verbascoside complex was stable around 2 Å after 4000 ps. In the 6jyg-verbascoside complex structure, it was observed that the ligand was more stable, especially after 2000 ps, and the RMSD value was smaller than the other system and was around 1 Å. Both ligands and protein structures were found to be stable and RMSD values were within acceptable values (<2.0 Å) (Figure 9).

The R_G of a protein is a measure of its compactness. If a protein is stably folded, it will probably maintain a relatively constant R_G value. If a protein unfolds, its R_G will change over time. A smaller R_G value indicates that the protein is more

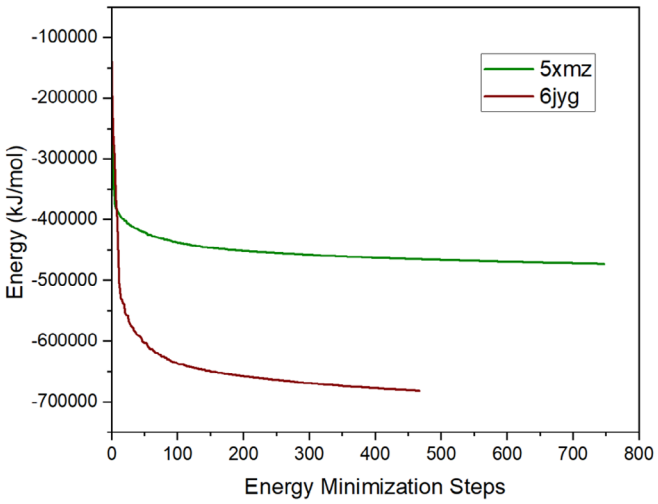

Figure 8. Potential energy change of the systems (protein + water + ions) obtained by energy minimization.

tightly wound and less mobile, while a larger value indicates that the protein is more loosely wound and more mobile.[43] Root mean square fluctuation (RMSF) is a measure of fluctuations in the position of each amino acid of a protein. RMSF is used to measure the local flexibility of a protein and is an ideal metric for comparing mobility in different regions of the protein. Higher RMSF values indicate more mobility in that region of the protein, while lower RMSF values indicate less mobility in that region. Optionally, the RMSF of C_α atoms is also computed.[44] In the simulation of the 5xmz-verbascoside complex, the R_G values did not change reasonably between 1000 and 9000 ns and were more stable in this range, while the R_G values of the 6jyg-verbascoside complex did not change much during the simulation. This indicates that the 6jyg-verbascoside system is more stable than 5xmz-verbascoside (Figure 10a). The average R_G values for 5xmz-verbascoside and 6jyg-verbascoside complexes were calculated as 1.49 and 1.94 nm, respectively. When the RMSF plots of the complexes formed by the ligands with the protein were analyzed, it was observed that the fluctuations of the critical residues of the 5xmz-verbascoside complex were around 0.25 Å and 0.6 Å, while those of the PBB-protein complex were around 0.15 Å and 0.2 Å (Figure 10b). These calculations can be used as an important measure to support that the ligands in these regions show stable interactions with the binding site of the protein.

Figure 11a, b shows the temperature-time and pressure-time graphs of both systems during 10 000 ps. In the equilibrium step lasting 10 000 ps under constant pressure, constant temperature, and constant molecule number conditions according to the pressure-time graph we obtained, although there are large oscillations in pressure values during this period, these oscillations are around 1 bar and the average pressure values are 1.10 for 5xmz-verbascoside and 1.03 bar for 6jyg-verbascoside. Likewise, in the temperature-time graph although there are fluctuations in temperatures throughout the simulation, the temperature of both systems varies around 300 K. The average temperatures of 5xmz-verbascoside and 6jyg-verbascoside systems during the simulation are 299.99 K and 299.98 K, respectively. The average temperature and pressure values of both systems show that the simulations are in a good equilibrium state.

The time dependence of the number of hydrogen bonds between verbascoside ligand and proteins is shown in Figure 12 with red-colored lines. In the 5xmz-verbascoside system, the hydrogen bonds between the ligand and the protein increase between 1000 and 3500 ps during the simulation period, while they tend to remain constant between 4000 and 10000 ps. In the 6jyg-verbascoside system, the hydrogen bonds between the ligand and the protein tend to remain constant between 1000 and 6500 ps during the simulation period, while they tend to decrease between 8000 and 10000 ps. As can be seen from the graph, the 6jyg-verbascoside system had more hydrogen bonding interactions than the 5xmz-verbascoside system throughout the simulation.

Coul-SR (Coulombic short-range) and LJ-SR (Lennard-Jones short-range) energies are terms used to calculate the potential energy of a molecule. This energy is calculated based on

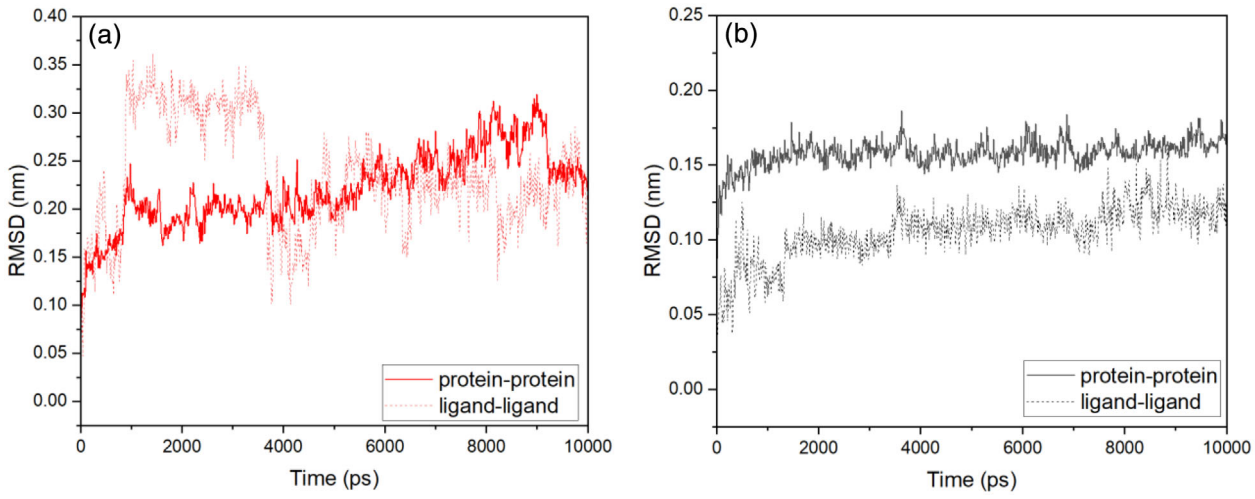

Figure 9. RMSD plot of protein-protein and ligand-ligand interactions of (a) 5xmz-verbascoside and (b) 6jyg-verbascoside complexes.

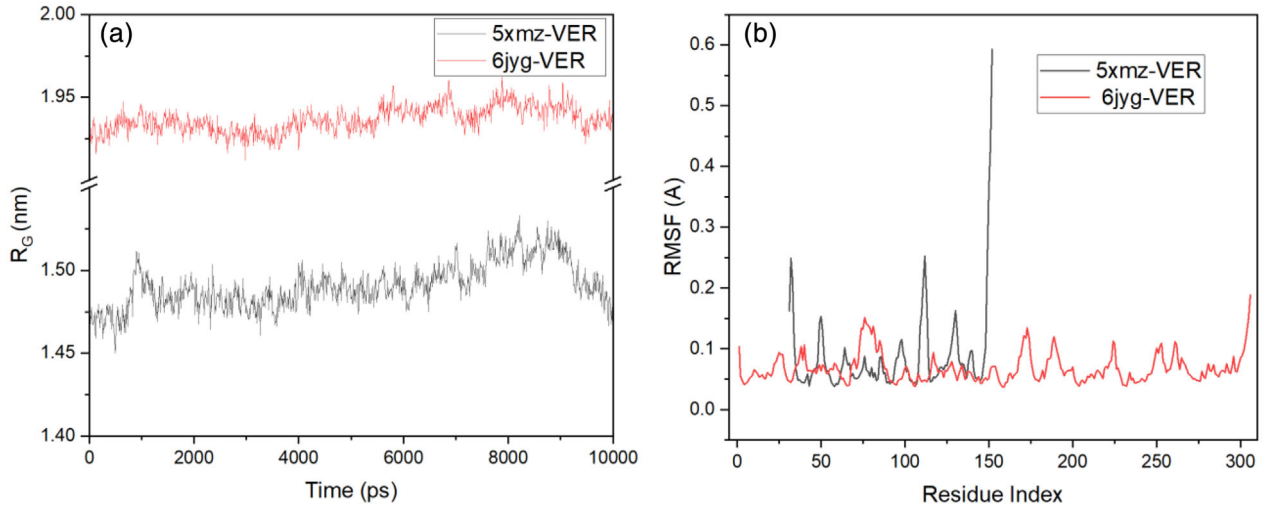

Figure 10. (a) R_G (b) RMSF plot of complex structures.

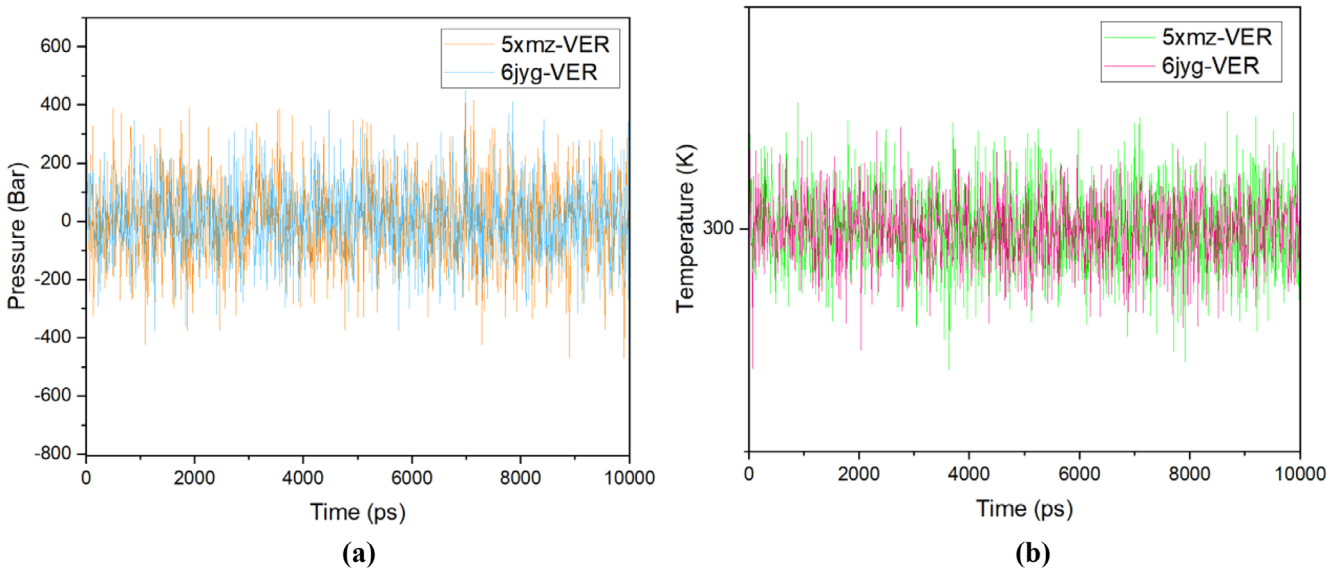

Figure 11. (a) Pressure and (b) temperature plots of complex structure.

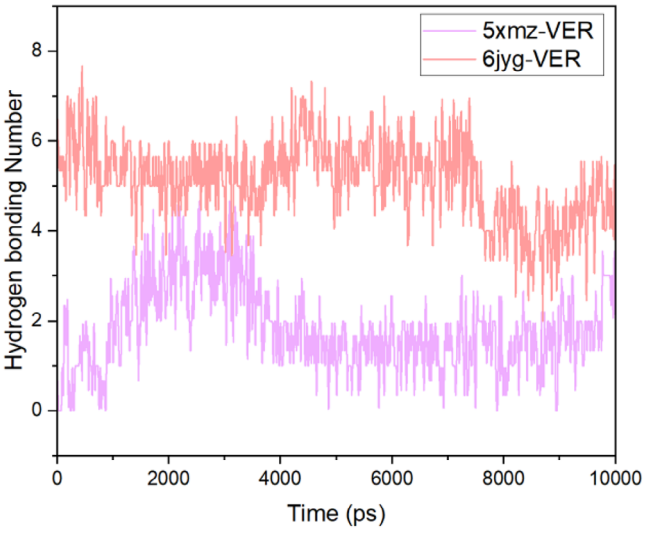

Figure 12. Hydrogen bonding number vs simulation time.

the Coulomb force law and measures electrostatic interactions between molecules. LJ-SR energy is the energy resulting from the molecule's van der Waals interactions. This energy is calculated based on the Lennard-Jones potential function and measures van der Waals interactions between molecules. Both energies are related to the interactions of molecules and the sum of these energies is used when calculating the potential energy of a molecule. Ligand-protein interaction energies were measured with short-range (SR), Lennard-Jones, (LJ-SR), and Coulomb (Coul-SR) potentials. The mean Coul-SR total interaction energies of the 5xmz-verbascoside and 6jyg-verbascoside complexes are −77.14 ± 25.84 and −206.12 ± 38.62 KJ/mol, while the mean LJ-SR total interaction energies are −119.86 ± 19.94 and −203.70 ± 18.20 KJ/mol, respectively. The averages of the total interaction energies of both systems were calculated as −197.00 ± 36.10 for 5xmz-verbascoside and −409.83 ± 35.70 kJ/mol for 6jyg-verbascoside (Figure 13). This indicates that the 6jyg-verbascoside system has a more stable structure.

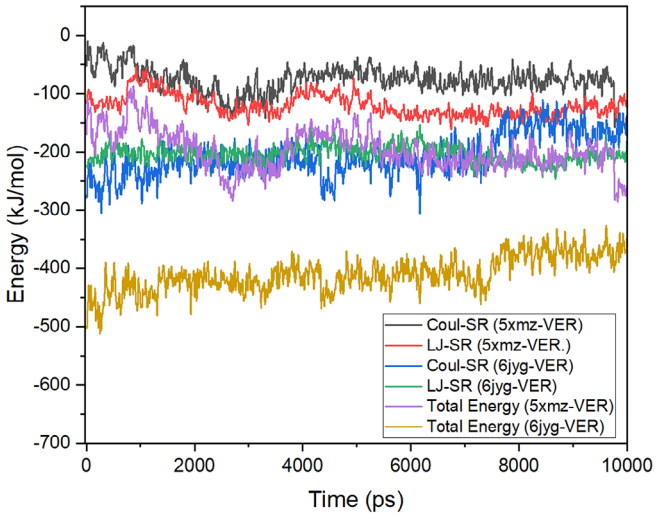

Figure 13. Short-and long-range interaction and total energies of complex structures.

3.5. Binding Free Energy Calculations

There is much literature on binding free energy.[45–47] The free energy of binding refers to the change in the free energy of a molecule during binding to another molecule or ligand. This energy change is the difference in free energy due to the association of energy and structural changes. The binding free energy is calculated by the following Equation (1):[45,48]

$$\Delta G_{bind} = -RT \ln (K_d) \quad (1)$$

where R is the gas constant; T is the absolute temperature; and K_d is the dissociation constant (dissociation constant, which is the inverse of binding). The free energy of binding can also be calculated using the relationship between the enthalpy of binding ΔH_{bind} and the entropy of binding ΔS_{bind} Equation (2):[47]

$$\Delta G_{bind} = \Delta H_{bind} - T\Delta S_{bind} \quad (2)$$

The MM/PBSA (Mechanical Poisson-Boltzmann surface area) method calculates the binding energy using molecular dynamics simulations and structure-based energy minimization methods. g. mmpbsa is a Gromacs tool used to calculate the free energy of a molecule in solution. MMPBSA (Molecular Mechanics/Poisson-Boltzmann Surface Area) is a method used to calculate the thermodynamic properties of a protein-ligand complex. This method is used to calculate different components of a protein-ligand complex such as binding energy, hydrophobic interactions, electrostatic interactions, and solvent interactions. g mmpbsa tool uses Gromacs output files to apply the MMPBSA method and calculates different properties to analyze the results. This tool is used in many fields such as drug discovery and design.[48,49]

The MM/PBSA (Molecular Mechanics Poisson-Boltzmann Surface Area)[50] method calculates the protein-ligand binding free energy with the following Equation (3):[51]

$$\Delta G_{bind} = \Delta E_{MM} + \Delta G_{polar} + \Delta G_{nonpolar} - T\Delta S \quad (3)$$

here ΔE_{MM} is defined as the minimum energy of the complex; ΔG_{polar}, polar solvation free energy; $\Delta G_{nonpolar}$, a polar solvation free energy; T is temperature; ΔS is binding entropy. The binding free energies of the ligand-protein complexes and the calculated summary energies of the three components of these energies are given in Table 4 and 5. Also the changes of these energies over 10,000 ps are shown graphically in Figures 14 and 15.

When we look at the results, the Binding free Energy value of the complex structure formed by the synthesized ligand with the 6jyg protein was larger than the 5xmz protein. This indicates that the binding of the ligand to the 6jyg receptor requires less energy and is in a more stable structure. Residue contribution energy is a term that provides information about the energy profile of a protein. The energy of a protein depends on many factors such as the binding of various amino acid residues, hydrophobic interactions, electrostatic interactions, hydrogen bonds, and so on. "Residue contribution energy" refers to the contribution of this energy to each amino acid residue. While this term provides insight into the thermodynamic behavior of a protein, it is also important for applications such as protein engineering and drug design. SASA (Solvent accessible surface area) is a frequently used method for calculating the surface area of protein structures. This calculation calculates the surface area closest to the state of the protein in solution and therefore accurately reflects the contribution of the protein's polar, apolar, and charge-carrying amino acids. SASA helps to understand many biochemical processes such as protein folding thermodynamics, protein-protein, and protein-ligand interactions.[52] The residues contributing to the binding free energy are given in Figure 16. The graphs show that the 5xmz-verbascoside complex shows the regions where the polar interaction with the solvent is intense with between residues 103–115. Likewise, the 6jyg-verbascoside complex shows a larger contribution to the energy in the polar interaction with between residues 33–37.

Table 4. Summary Energy (kJ/mol) of 5xmz-verbascoside complex.

van der Waal energy	−159.877 ± 16.858 kJ/mol
Electrostatic energy	−63.601 ± 16.748
Polar solvation energy	182.353 ± 26.979
SASA energy	−17.750 ± 1.619
Binding free energy	−58.875 ± 19.470

Table 5. Summary Energy (kJ/mol) of 6jyg-verbascoside complex.

van der Waal energy	−196.910 ± 17.904
Electrostatic energy	−100.643 ± 22.468
Polar solvation energy	248.879 ± 31.095
SASA energy	−24.034 ± 1.336
Binding free energy	−72.708 ± 19.580

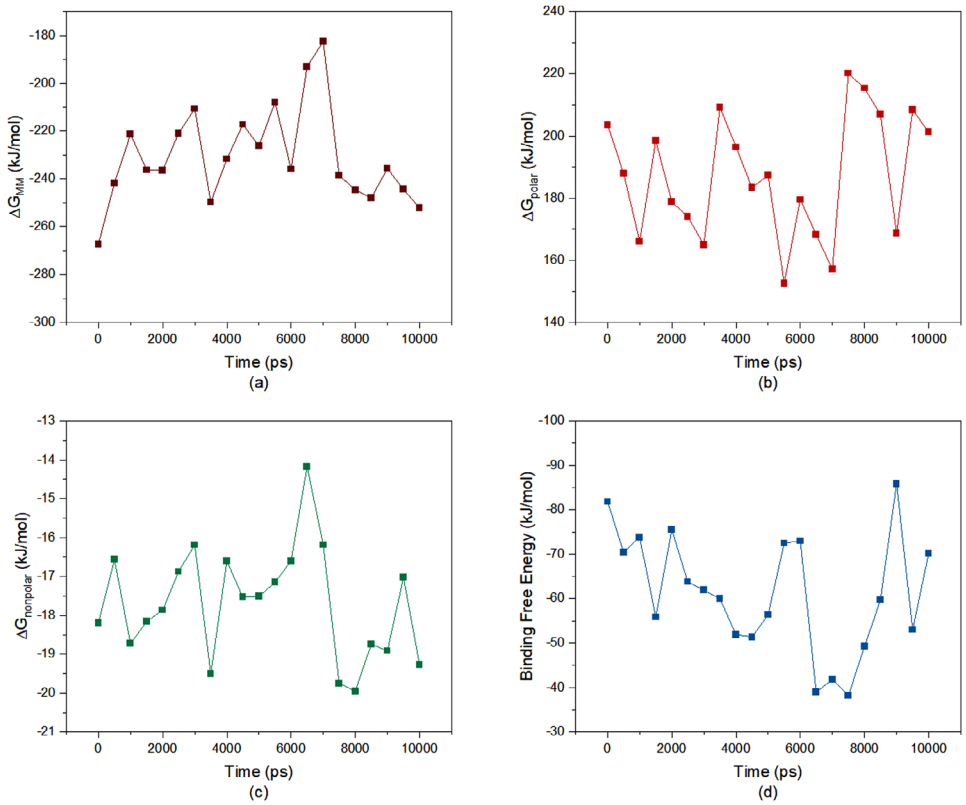

Figure 14. Energy components of 5xmz-verbascosidecomple; (a) The potential energy in the vacuum. (b) Polar solvation energy. (c) Nonpolar solvation energy. (d) Binding Free energy. ΔG: change in free energy, MM: molecular mechanics.

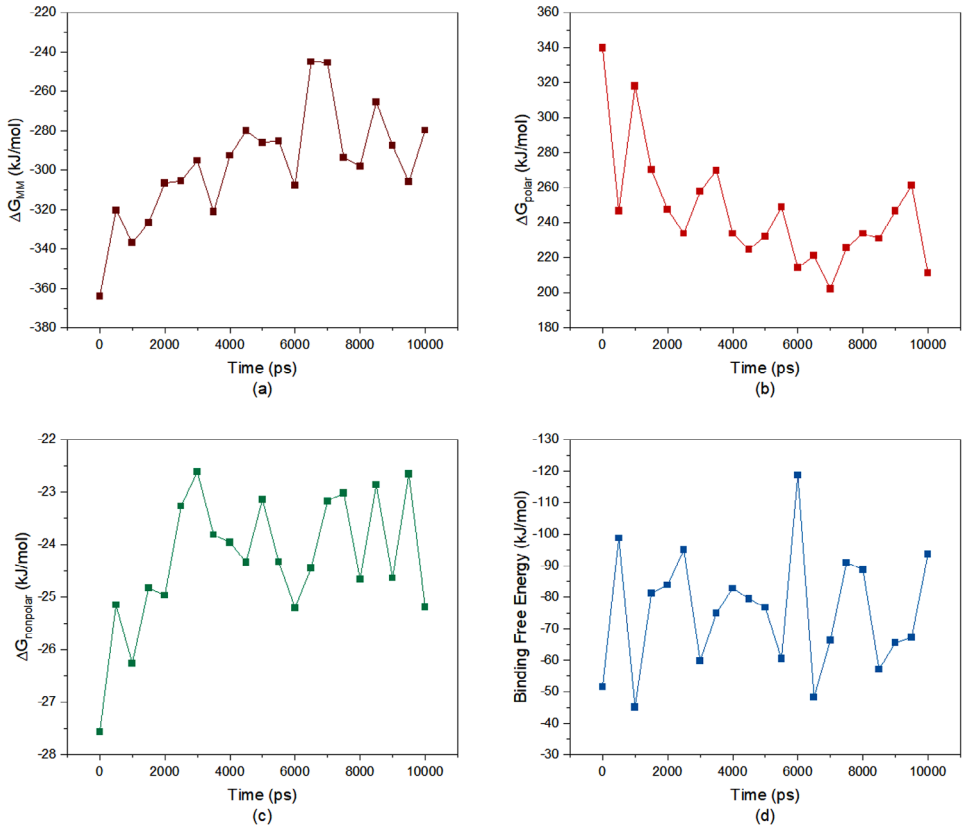

Figure 15. Energy components of the 6jyg-verbascoside complex; (a) The potential energy in the vacuum (b) Polar solvation energy. (c) Nonpolar solvation energy. (d) Binding Free energy. ΔG: change in free energy, MM: molecular mechanics.

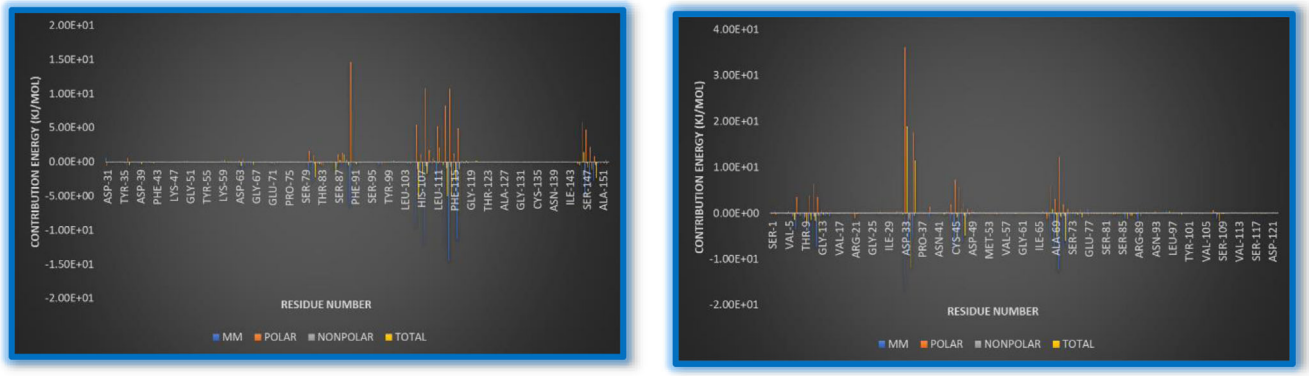

Figure 16. Residue contribution energies of (a) 5xmz-verbascoside (b) 6jyg-verbascoside complexes.

In our study, molecular docking and dynamic simulation methods were employed to investigate the antifungal activity of Verbascoside against *V. dahliae* (PDB: 6jyg) and *P. infestans* (PDB: 5xmz). The results demonstrated that Verbascoside exhibits strong binding affinities to the active sites of these fungal proteins with key amino acid interactions identified through residue contribution energy analysis. Notably, MM/PBSA calculations confirmed the energetic favorability of these interactions further supporting the stability of the ligand-protein complexes under simulated conditions. This approach aligns with earlier studies, such as the molecular docking analysis of the SARS-CoV-2 main protease (PDB: 6LU7, 6Y84),[53] where hydrogen bonding and $\pi-\pi$ interactions with key amino acids in the active site were highlighted. Similarly, in our study critical interactions between Verbascoside and amino acids like Asp and Tyr within the binding pockets were observed underscoring the ligand's high affinity and potential as an inhibitor. Additionally, our work shares methodological similarities with the docking studies on HCV NS3 protease inhibitors.[54] These studies emphasized the significance of electrostatic interactions within the negatively charged binding pockets of the protease. Correspondingly, our study provided detailed insights into the electrostatic complementarity and stabilization of Verbascoside within its target proteins. These findings collectively reinforce the potential of natural compounds like Verbascoside as promising candidates for antifungal and antiviral drug development.

4. Conclusions

This study provides the first evaluation of the antifungal activity of verbascoside against the pathogens *P. infestans* and *V. dahliae*. Verbascoside demonstrated moderate inhibitory effects on mycelial growth in vitro assays reducing growth by 23.49% and 19.42% for *P. infestans* and *V. dahliae* at 2 mg/mL, respectively. These results highlight the potential of verbascoside as a natural antifungal agent.

To further understand its mode of action, in silico molecular docking and molecular dynamics simulations were employed. The simulations revealed that verbascoside forms stable interactions with target proteins particularly with the 6jyg protein structure of *P. infestans*, as indicated by favorable binding free energy values and consistent structural stability. The detailed analysis of molecular interactions including hydrogen bonding and van der Waals forces supports the hypothesis that verbascoside can disrupt critical protein functions in these pathogens.

By integrating in vitro and in silico methodologies, this study establishes a foundation for the development of eco-friendly antifungal agents derived from plant metabolites. While the findings are promising future research should focus on optimizing the efficacy of verbascoside exploring its synergistic effects with other bioactive compounds and conducting field trials to validate its application in agriculture. This method could decrease dependence on synthetic fungicides reducing their environmental and health effects.

Author Contributions

Yusuf Bayar contributed to antifungal studies, evaluation, analysis of data, and preparation of article draft. Samed Şimşek, Hüseyin Akşit contributed to the development of the verbascoside isolation method. Tuncay Karakurt carried out molecular docking and molecular docking simulation studies. All the authors revised the final manuscript and approved the submission.

Acknowledgments

The authors have nothing to report.

Conflict of Interests

The authors declare no conflict of interest.

Data Availability Statement

The data that support the findings of this study are available in the supplementary material of this article.

Keywords: Antifungal activity · Molecular docking simulations · Verbascoside · *Verbascum ozturkii*

[1] S. Şimşek, H. Akşit, A. Aydın, E. Köksal, *Chem. Biodivers.* **2023**, *20*, e202301200.
[2] E. Tuzlacı, *Marmara Pharm. J.* **2006**, *14*, 47–52.
[3] F. Senatore, D. Rigano, C. Formisano, A. Grassia, A. Basile, *Fitoterapia.* **2007**, *78*, 244–247.
[4] E. K. Akkol, I. I. Tatli, Z. S. Akdemir, *Z Naturforsch C J Biosci* **2007**, *62*, 813–820.
[5] H. A. E. H. El Gizawy, M. A. Hussein, E. Abdel-Sattar, *Pharm. Biol.* **2019**, *57*, 485–497.
[6] A. Gökmen, N. Kúsz, N. Karaca, F. Demirci, J. Hohmann, H. Kırmızıbekmez, *Nat. Prod. Res.* **2021**, *35*, 5294–5298.
[7] H. Y. Gondal, Z. Roshan, N. Muhammad, C. Muhammad, *Nat. Prod. J.* **2020**, *10*, 158–162.
[8] M. I. Georgiev, K. Ali, K. Alipieva, R. Verpoorte, Y. H. Choi, *Phytochemistry* **2011**, *72*, 2045–2051.
[9] B. Klimek, M. A. Olszewska, M. Tokar, *Phytochem. Anal.* **2010**, *21*, 150–156.
[10] G. Fu, H. Pang, Y. H. Wong, *Curr. Med. Chem.* **2008**, *15*, 2592–2613.
[11] F. A. Karaveliogullari, M. E. Uzunhisarcikli, S. Celik, *Pak. J. Bot.* **2008**, *40*, 1595–1599.
[12] K. Alipieva, L. Korkina, I. E. Orhan, M. I. Georgiev, *Biotechnol. Adv.* **2014**, *32*, 1065–1076.
[13] M. D'Imperio, A. Cardinali, I. D'Antuono, *Food Res. Int. 66*, 373–378.
[14] A. M. Díaz, M. J. Abad, L. Fernández, A. M. Silván, J. De Santos, P. Bermejo, *Life Sci.* **2004**, *74*, 2515–2526.
[15] M. Georgiev, K. Alipieva, I. Orhan, R. Abrashev, P. Denev, M. Angelova, *Food Chem.* **2011**, *128*, 100–105.
[16] G. R. Pettit, A. Numata, T. Takemura, R. H. Ode, A. S. Narula, J. M. Schmidt, G. M. Cragg, C. P. Pase, *J. Nat. Prod.* **1990**, *53*, 456–458.
[17] M. Georgiev, S. Pastore, D. Lulli, K. Alipieva, V. Kostyuk, A. Potapovich, M. Panetta, L. Korkina, *J. Ethnopharmacol.* **2012**, *144*, 754–760.
[18] C. S. Funari, F. P. Gullo, A. Napolitano, R. L. Carneiro, M. J. Mendes-Giannini, A. M. Fusco-Almeida, S. Piacente, C. Pizza, D. H. Silva, *Food Chem.* **2012**, *135*, 2086–2094.
[19] A. K. Nikonorova, C. A. Egorov, T. G. Galkina, E. V. Grishin, A. V. Babakov, *Mikol. Fitopatol.* **2009**, *43*, 52–57.
[20] J. N. Oyourou, S. Combrinck, T. Regnier, A. Marston, *Ind. Crops Prod.* **2013**, *43*, 820–826.
[21] Ç. Kahraman, i.i. Tatli, D. Kart, M. Ekizoğlu, Z. Ş. Akdemir, *Turk. J. Pharm. Sci.* **2018**, *15*, 231–237.
[22] N. Ü. Turan, H. U. Çelebioğlu, H. Akşit, R. Taş, *Biotech. Studies* **2020**, *29*, 47–54.
[23] M. O. Nwosu, J. I. Okafor, *Mycoses* **1995**, *38*, 191–195 p..
[24] D. K. Pandey, N. N. Tripathi, R. D. Tripathi, S. N. Dixit, *J. Plant Dis. Prot.* **1982**, *89*, 344–349.
[25] A. D. Becke, *J. Chem. Phys.* **1992**, *96*, 2155–2160.
[26] C. Lee, W. Yang, R. G. Parr, *Phys. Rev. B 37*, 785–789.
[27] J. Foresman, A. Frisch, *Exploring chemistry with electronic structure methods: A guide to using Gaussian*, Gaussian Inc, Pittsburgh, PA **1996**.
[28] M. Frisch, G. W. Trucks, H. B. Schlegel, G. E. Scuseria, M. A. Robb, J. R. Cheeseman, G. Scalmani, V. P. G. A. Barone, B. Mennucci, G. A. Petersson, H. Nakatsuji, Gaussian 09, Revision a. 02, 200, gaussian. Inc., Wallingford, CT **2009**, p. 271.
[29] R. Dennington, T. Keith, J. Millam, GaussView, version 5 **2009**.
[30] E. F. Pettersen, T. D. Goddard, C. C. Huang, G. S. Couch, D. M. Greenblatt, E. C. Meng, T. E. Ferrin, *J. Comput. Chem.* **2004**, *25*, 1605–1612.
[31] O. Trott, A. J. Olson, *J. Comput. Chem.* **2010**, *31*, 455–461.
[32] M. J. Abraham, T. Murtola, R. Schulz, S. Páll, J. C. Smith, B. Hess, E. Lindahl, *SoftwareX* **2015**, *1*, 19–25.
[33] R. Kumari, R. Kumar, A. Lynn, *J. Chem. Inf. Model.* **2014**, *54*, 1951–1962.
[34] M. Elmastas, R. Erenler, B. Isnac, H. Aksit, O. Sen, N. Genc, I. Demirtas, *Nat. Prod. Res.* **2016**, *30*, 299–304.
[35] S. Demirci, C. Alp, H. Akşit, Y. Ulutaş, A. Altay, E. Yeniçeri, E. Köksal, N. Yayh, *Chem. Biol. Drug Des.* **2023**, *101*, 1273–1282.
[36] P. Magiatis, S. Mitaku, E. Tsitsa, A. L. Skaltsounis, C. Harvala, *Nat Prod Lett* **1998**, *12*, 111–115.
[37] Z. Akdemir, C. Kahraman, I. I. Tatlı, E. Küpeli Akkol, I. Süntar, H. Keles, *J. Ethnopharmacol.* **2011**, *136*, 436-443.
[38] J. N. Oyourou, S. Combrinck, T. Regnier, A. Marston, *Ind. Crops Prod.* **2013**, *43*, 820–826.
[39] E. Shikanga, T. Regnier, S. Combrinck, B. Botha, *Fruits* **2009**, *64*, 75–82.
[40] I. leming, *Molecular orbitals and organic chemical reactions*, John Wiley & Sons, New York City, USA, **2011**.
[41] L. T. Nagy, V. Mocko, *Gen. Physiol. Biophys.* **1984**, *3*, 339–345.
[42] D. Case, *AMBER*, University of California, San Francisco **2018**.
[43] P. Godara, B. Naik, R. Meghwal, R. Ojha, V. Srivastava, V. K. Prajapati, D. Prusty, *Life Sci.* **2022**, *311*, 121121.
[44] P. Rao, A. Shukla, P. Parmar, R. M. Rawal, B. Patel, M. Saraf, D. Goswami, *Biophys. Chem.* **2020**, *264*, 106425.
[45] M. K. Gilson, J. A. Given, B. L. Bush, J. A. McCammon, *Biophys. J.* **1997**, *72*, 1047–1069.
[46] P. Kollman, *Chem. Rev.* **1993**, *93*, 2395–2417.
[47] A. R. Leach, *Molecular modelling: principles and applications*, Prentice Hall, Englewood Cliffs **2001**.
[48] M. R. Şhirts, J. D. Chodera, *J. Chem. Phys.* **2008**. 129.
[49] R. Kumari, R. Kumar, *J. Chem. Inf. Model.* **2014**, *54*, 1951–1962.
[50] P. A. Kollman, I. Massova, C. Reyes, B. Kuhn, S. Huo, L. Chong, M. Lee, T. Lee, Y. Duan, W. Wang, O. Donini, P. Cieplak, J. Srinivasan, D. A. Case, *Acc. Chem. Res.* **2000**, *33*, 889–897.
[51] Z. Yang, F. Wu, X. Yuan, L. Zhang, S. Zhang, *J Mol Graph Model* **2016**, *65*, 27–34.
[52] B. Lee, F. M. Richards, *J. Mol. Biol.* **1971**. *55*, 379–400.
[53] M. A. Hosen, N. S. Munia, M. Al-Ghorbani, M. Baashen, F. A. Almalki, T. B. Hadda, S. M. Kawsar, *Bioorg. Chem.* **2022**, *125*, 105850.
[54] H. Lafridi, F. A. Almalki, T. Ben Hadda, M. Berredjem, S. M. Kawsar, A. M. Alqahtani, H. Zgou, *J. Biomol. Struct. Dyn.* **2023**, *41*, 2260–2273.

Manuscript received: February 12, 2024